Hindawi
International Journal of Antennas and Propagation
Volume 2021, Article ID 6638096, 10 pages
https://doi.org/10.1155/2021/6638096

Research Article

Design of Planar Microstrip Ultrawideband Circularly Polarized Antenna Loaded by Annular-Ring Slot

Zhong-Hua Ma,[1] **Jia-Xiang Chen**,[1] **Peng Chen**,[1] **and Yan Feng Jiang**[2]

[1]*College of Information Engineering, Jimei University, Xiamen 361021, China*
[2]*College of IoT Engineering, Jiangnan University, Wuxi 214122, China*

Correspondence should be addressed to Yan Feng Jiang; jiangyf@jiangnan.edu.cn

Received 30 December 2020; Revised 18 February 2021; Accepted 10 March 2021; Published 17 March 2021

Academic Editor: Giuseppina Monti

A miniaturized planar microstrip circularly polarized ultrawideband (UWB) antenna loaded by annular-ring slot is proposed and implemented in the paper. With the annular-ring slot loaded in the radiating patch of the antenna, the side of the radiating patch is connected by the asymmetric inverted *L*-shaped microstrip. At the same time, a quarter of a circle is cut off from the radiating patch. The above designed structure shows improvements on the operating frequency band and realization of the circular polarization radiation. A tapered microstrip is placed between the feed line and the radiating patch to achieve the slow-changing impedance transformation. The results of simulation and measurement demonstrate that the 3 dB axial ratio (AR) fractional bandwidth of the antenna structure achieves 21.25%. The peak gain within the 3 dB axial ratio bandwidth fluctuates between 3.74 and 4.59 dBi. The antenna shows good impedance matching in the ultrawideband range. With the compact structure of the UWB antenna, it has potential application in various wireless communication devices.

1. Introduction

In recent years, the rapid developments of the radio frequency and microwave integrated circuit technology drive the continuous increment in various wireless communication systems such as satellite communications, mobile communications, and wireless sensor networks. Multiple communication systems usually coexist in the single mobile devices, while their operating frequency bands are strictly required to be separated from each other. So multiple antennas are always needed in the system to fulfill the transceiver services.

However, due to the space limitation in the mobile devices, it is difficult to integrate multiple antennas in a single system. Moreover, the integration of the multiple antennas brings about the coupling effects among the antennas, which could degrade the receiving sensitivity and signal-to-noise ratio. The above problems severely degrade the characteristics of the system and bring about the difficulties in the design of the antennas and the radio frequency (RF) circuit front-ends.

The ultrawideband (UWB) should be one of the possible solutions for the multiantenna system, since its wideband covers many communication applications. At the same time, its size can be minimized in small volume without the coupling effect [1–3]. However, the application of the UWB antenna is still limited because of the linear polarization (LP) characteristics of the UWB antenna. To solve the problem, the circular polarization (CP) antenna attracts more and more interests with its benefits such as reducing multipath effects, enhancing signal reliability, reducing polarization losses between transmitting and receiving antennas, and optimizing the weakness of antenna directivity. Based on the above advantages, UWB CP antennas are widely used in wireless communication systems [4–10].

With its excellent characteristics, the CP antenna is used widely in various application scenarios. For example, it is used in the radar systems to prevent the interference of clouds and rains [4]. In electronic countermeasures, the CP antennas can interfere with and detect various linear polarized and elliptical polarized radio waves [5]. In the aircraft

with the harsh environment, the CP antenna can receive the information correctly [6, 7]. In the television broadcasting system, the CP antenna can overcome the ghosting problem [8]. With these benefits, many research studies on the CP UWB antennas are conducted and various structures are proposed and designed recently. Reference [9] proposes an UWB antenna based on crossed magnetoelectric dipoles. The electric dipole is changed to a folded square ring to reduce the area and extend the current path. The CP is obtained by connecting a 90° hybrid coupler. The 3 dB axial ratio (AR) fractional bandwidth is 1.7 GHz. A horn dual-circularly polarized broadband millimeter wave antenna based on a waveguide spacer polarizer is proposed in [10]. The antenna can simultaneously transmit and receive two orthogonal CP waves to achieve duplex. Both of the two structures show good CP radiation performance [9, 10], wide AR bandwidth, and high gain. However, the above antennas are three-dimensional structure (3D), with the complicated structure, big size, and difficult manufacturing approach. Their current appearances are not suitable to be used in mobile devices.

The impedance bandwidth is one of the key aspects in the UWB antenna. To improve the impedance bandwidth, the microstrip patches are integrated in the UWB antenna by reducing the quality factor. The integrated structure shows many merits, including low profile, light weight, simple structure, easy integration, and low manufacturing cost. The CP antenna with a single feed has a narrower AR bandwidth. In [11], the tilted-D-shaped radiator combined inverted-C-shaped microstrip structure and tilted-I-type microstrip structure are designed to obtain the CP characteristics. The radiator is connected with the 50 Ω transmission line through an impedance transformer. The upper and lower frequency bands realize the left-handed CP and the right-handed CP, respectively. The CP characteristic of this antenna exhibits excellently, and the 3 dB AR fractional bandwidth achieved is 31.16% and 22.62%. However, the area is still too large to be accepted in the mobile devices.

The area of the antenna is one of the key issues in the system design. To reduce the area, one of the feasible approaches is the adoption of the slot structures. The slots can be loaded on the radiation patch to reduce the area of the antenna and to increase the circumference of the antenna. By the adoption, changing the path of the antenna surface current is changed and good CP characteristics can be realized. In [12], the folded square ring slot is used to excite the CP field. The CP performance is improved by cutting a pair of grooves along the square patch border. However, the antenna in [12] needs a double-layer dielectric substrate, which increases the complexity and manufacturing difficulty of the antenna. In [6], the *L*-shaped microstrip is used to connect with the feed line. The *L*-shaped microstrip-line-feed is electromagnetically coupled to the two orthogonal sides of the square ring slot to achieve the CP. The antenna shows large area and low peak gain. Reference [13] uses single-port double-feed double-bent microstrip line feed to achieve the CP radiation. However, its size is not suitable for the compact system. In order to increase the 3 dB AR bandwidth of CP antenna, an annular slot and a cross slot are applied on the CP antenna in [14], in which the two slots lead two different frequency bands, separately. The asymmetry is introduced to the annular slot and the cross slot, which can obtain the CP radiation at two frequencies. Reference [15] proposes a C-shaped grounded microstrip dual-frequency coplanar waveguide-fed annular slot antenna, which achieves CP through two diagonally loading slots. The horizontal length of the C-shaped grounded strip can be adjusted for the improvement of the AR fractional bandwidth. Reference [16] shows dual-induction CP by adjusting the inner and outer radius of the annular slot and increasing the length of four unequal linear slots of the annular slot. The size is 80 mm × 80 mm. The AR bandwidth is only greater than 6%. The study in [17] uses a single microstrip feed to realize a printed spiral slot defected ground structure (DGS) dual-frequency CP antenna. An additional embedded spiral slot is introduced in the backside of the antenna to improve the AR fractional bandwidth. The hybrid coupler feeding method is adopted to achieve wide AR bandwidth. However, the size and the loss are increased accordingly. A circularly polarized square slot antenna is proposed in [18]. The CP excitation is generated with embedding *L*-shaped microstrips of unequal sizes near two diagonal corners in a square slot. The impedance bandwidth is 10.2 GHz and the CP fractional bandwidth is 32.3%. However, the radiation pattern is not good enough for the application.

The CP antenna of the single-port double-feed structure is relatively complicated feeding structure, in which the slight perturbation structure in the antenna in conjunction with the single-port double-feed structure is included [13, 19, 20]. A hybrid coupler with a balanced microstrip feed line is one of the best candidates for CP, but it is very difficult to match the input impedance of the balanced line. Furthermore, the length of the feed line is increased. Currently, much attention is given to using a single layer to reduce the size of the microstrip antenna.

In this paper, a facile microstrip planar single-port single-feed UWB CP antenna structure is proposed and implemented. A quarter of a circle is cut off from the one corner of the rectangular microstrip radiating patch. A tapered microstrip is used to connect the radiating patch with the feed line as the impedance matching slowly transition structure. An annular-ring slot is loaded on the patch near the feed line for the excitation of the CP. An unbalanced inverted *L*-shaped microstrip is applied for the adjustments of the AR value and the CP bandwidth. Detailed information on the proposed structure is reported in the following.

2. Antenna Structure

Figure 1 shows the structure diagram of the linear polarization (LP) UWB antenna. The rectangular radiating patch is connected with the feed line through the tapered microstrip. At the bottom of the substrate, there is a rectangular ground plate with the same length as the feed line. The FR4 substrate is used in the design, with the thickness of 1 mm, the relative dielectric constant of 4.4, and the loss tangent of 0.02. The size of the substrate is $24 \times 25\,\text{mm}^2$ and the size of the radiating patch is 12.5 mm × 15 mm. The width of the feed line

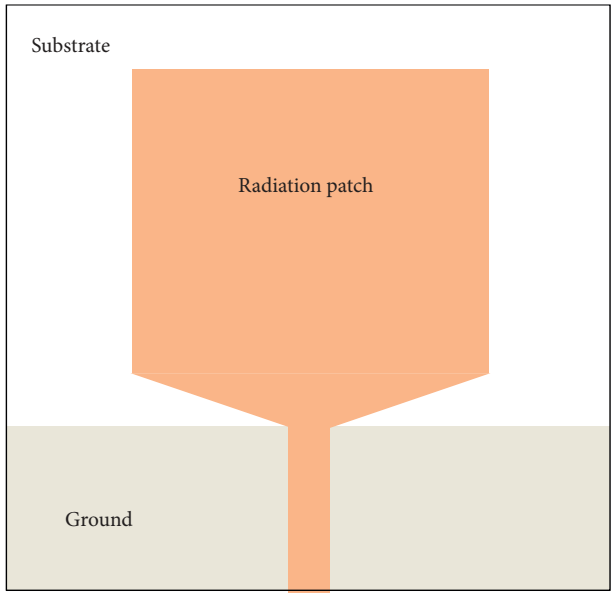

Figure 1: Schematic of the structure of the LP microstrip patch antenna.

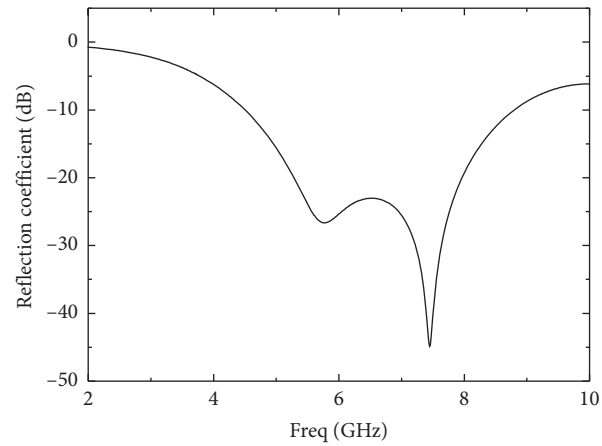

Figure 2: The reflection coefficient results of the antenna shown in Figure 1.

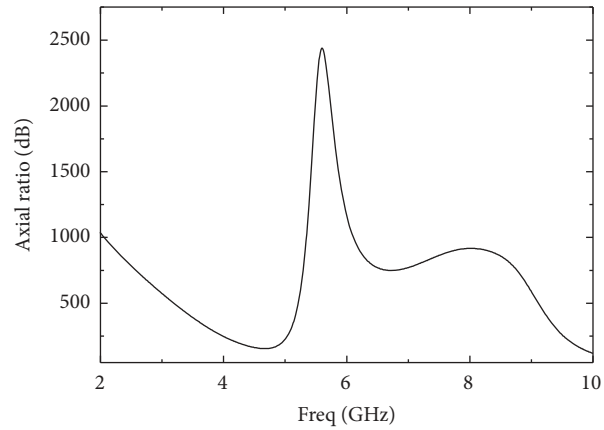

Figure 3: Simulation result of the AR of the structure in Figure 1.

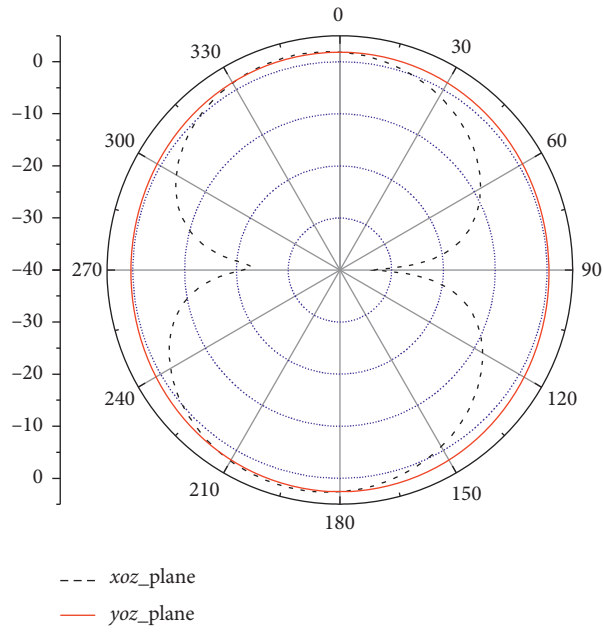

Figure 4: Simulated *xoz* plane and *yoz* plane radiation patterns at 6.5 GHz.

is 2.12 mm. Figure 2 is the reflection coefficient simulating curve based on the high-frequency electromagnetic simulation software (HFSS). The frequency band is from 4.52 GHz to 8.7 GHz when the reflection coefficient is less than −10 dB. The impedance bandwidth is 4.18 GHz.

Figure 3 is the graph of the AR of the antenna in Figure 1. The AR is much greater than 100 dB in 2 GHz to 10 GHz. Therefore, the structure is a LP UWB antenna. Figure 4 is the directional pattern of this LP antenna at 6.5 GHz. It has omnidirectional radiation performance on the *yoz* plane and the directional radiation in *xoz* plane.

Cutting corner, slot loading, the branch line loading, and other methods are used in order to realize CP radiation on the microstrip antenna. In this paper, a quarter of a circle is cut off at one corner of the rectangular radiating patch. The inverted L-shaped microstrip is connected with the radiation patch loading annular-ring slot to realize CP. The structure proposed in this paper is shown in Figure 5.

As shown in Figure 5, the size of the antenna is $W \times L = 22\,\text{mm} \times 24\,\text{mm}$, in which L is the length and W is the width. The antenna radiation patch is implemented on the top layer of the substrate. The tapered microstrip acts as the connection between the radiation patch and the feed line. The length of the ground plate on the bottom of the substrate is the same as the feed line. The radius of the annular-ring slot is r. The width of the gap is w_{slot}. The height of the tapered microstrip is g. The length of the inverted L microstrip is L_3 and L_4, respectively, and the width is w_3. The length of the radiation patch is L_1, and the width is w_1. The cut-out part is a quarter of the circle with a radius of R. The width of the feed line is w_2 and the length is L_2. The key parameters include the position of the annular-ring slot, the cutting-out quarter circle radius R, and the length of the L-shaped microstrip. The

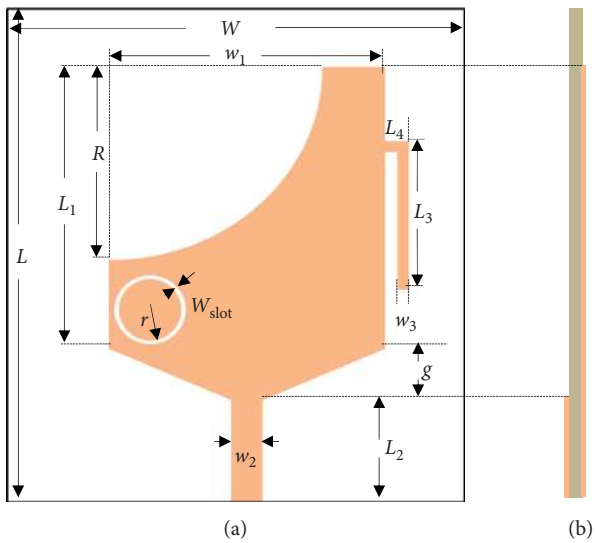

Figure 5: The structure of the proposed UWB CP antenna. (a) Top view. (b) Side view.

adjustments on these parameters can influence the AR. Therefore, CP radiation can be realized. In order to implement better impedance matching, the radiating patch is connected with the feed line by a tapered microstrip. The height of the tapered microstrip is set to be $g = 3$ mm. Table 1 shows the geometrical parameter values of this CP UWB antenna.

3. Circular Polarization

Figure 6 is the simulation result of the reflection coefficient curve of the CP. The values of the reflection coefficient between 4.52 GHz and 8.06 GHz are less than −10 dB. The impedance bandwidth achieves 3.54 GHz. Two poles can be observed in the band. The maximum reflection coefficient is 12.4 dB in the whole impedance band. The AR simulation curves of the CP UWB antenna are shown in Figure 7. The frequency region corresponding to the fact that the AR values are less than 3 dB is from 5.99 GHz to 7.1 GHz. The AR bandwidth is 1.11 GHz. Within the AR bandwidth, the input impedance of the antenna is close to the matching point of the Smith chart. At the lower edge frequency of the 3 dB AR bandwidth of 5.99 GHz, the input impedance of the antenna is $0.902 + j*0.372\ \Omega$. At the upper edge frequency of the 3 dB AR bandwidth of 7.10 GHz, the input impedance of the antenna is $0.885 + j*0.60\ \Omega$. At the center frequency of 6.5 GHz, the input impedance of the antenna is $1.171 + j*0.132\ \Omega$. Within the AR bandwidth range, the antenna impedance is close to the matching point. The imaginary part of the input impedance is relatively small, showing good system matching characteristic.

Figure 8 is the VSWR simulation curve of the UWB CP antenna. The frequency range is from 4.48 GHz to 8.13 GHz when the VSWR is kept less than 2, covering the range of 3 dB AR bandwidth. Furthermore, within the 3 dB AR bandwidth, the VSWR is less than 1.5.

Table 1: The geometrical parameters of the CP antenna (unit: mm).

r	R	W_{slot}	w_2	L_2	g	L_4	w_3	L_3	w_1	L_1	W	L	h
1.4	8	0.4	2.12	3.5	3	1	0.5	5	15	12.5	22	24	1

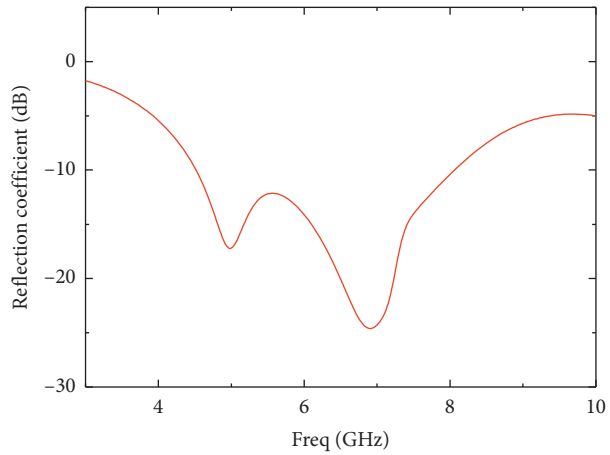

Figure 6: Simulation result of the reflection coefficient of the CP antenna.

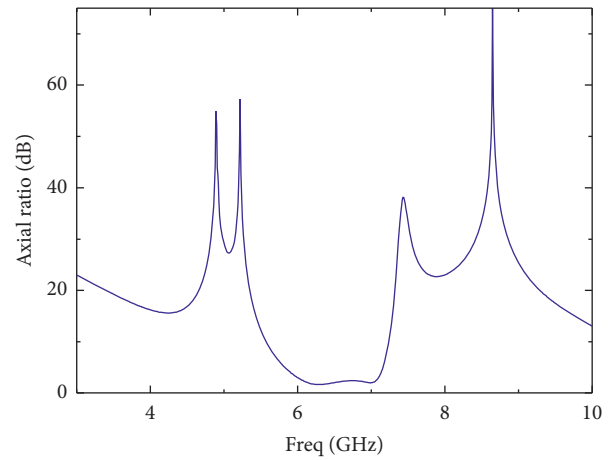

Figure 7: Simulation results of the axial ratio.

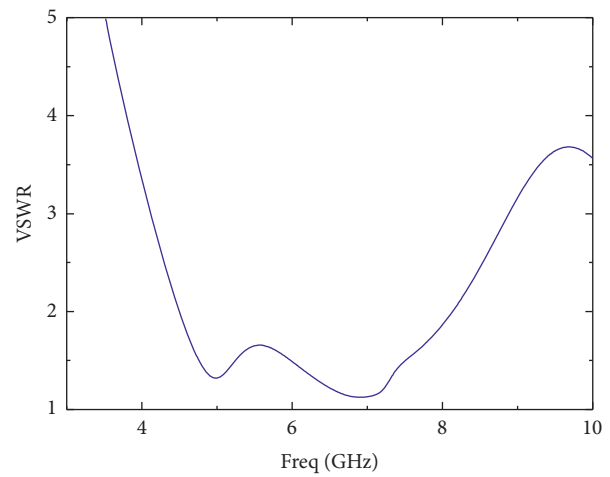

Figure 8: Simulation results of VSWR.

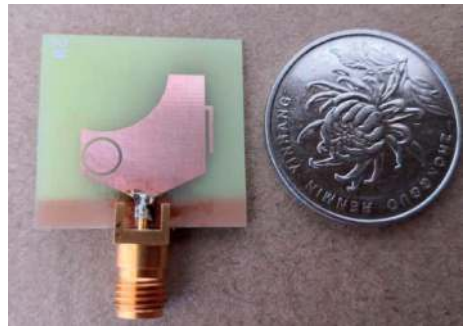

Figure 9: Photograph of the fabricated CP UWB antenna. A picture of coin is shown, giving a comparative observation on the actual size of the antenna.

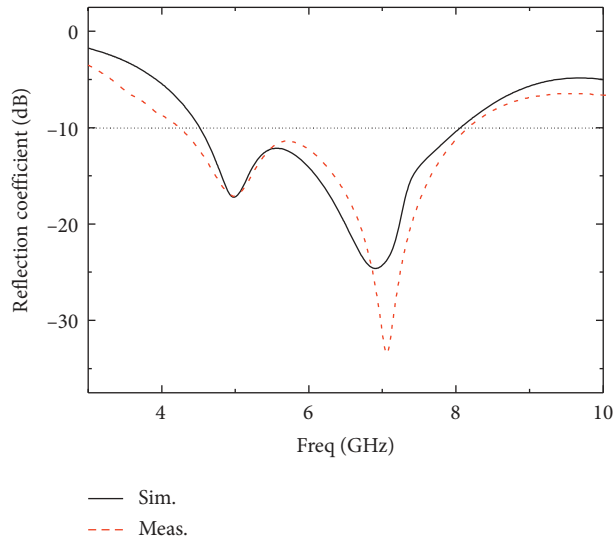

Figure 10: Measured reflection coefficient of the CP antenna. The solid line shows the simulation result, while the dashed line shows the measured ones.

4. Experiment Results

The CP UWB antenna is fabricated on the FR4 substrate. The photograph is shown in Figure 9. The CP antenna is characterized in the anechoic chamber. Its reflection coefficient is shown in Figure 10. The dashed line in Figure 10 is the measured result of the reflection coefficient. The frequency is from 4.25 GHz to 8.16 GHz with the reflection coefficient less than -10 dB. The impedance bandwidth achieves 3.91 GHz, which is slightly larger than the simulation result.

Figure 11 shows the measured *xoz* plane and *yoz* plane radiation patterns when the working frequencies are 6 GHz, 6.5 GHz, and 7 GHz, respectively. The radiation pattern has a little distortion because a quarter circle is cut off at one corner of the antenna radiation patch.

The measured VSWR, 3 dB AR, and gain curves are shown in Figures 12–14, respectively.

Figure 12 shows the measurement curve of the VSWR. The frequency is from 4.45 GHz to 8.36 GHz with the VSWR less than 2. Figure 13 is the measured AR curve. In Figure 13, the frequency region is from 5.9 GHz to 7.3 GHz with the AR less than 3 dB. The 3 dB AR bandwidth is 1.4 GHz and the 3 dB fractional bandwidth is 21.5%. The measurement curve of the CP antenna gain is shown in Figure 14. Within the 3 dB AR bandwidth, the gain fluctuates between 3.74 dBi and 4.59 dBi with relatively smooth variations. The characterization results demonstrate that the antenna shows good performance with the miniaturized structure.

5. Discussion

There are several structural parameters of the antenna which need to be adjusted to design the CP antenna. The CP performance is extremely sensitive to some parameters, thus increasing the design difficulty. In this paper, the key parameters, such as the radius and width of the annular-ring slot, the length of the inverted *L*-shaped microstrip, and the radius of the quarter circle, are discussed to study the influences on the antenna AR. With the annular-ring slot radius r changing, the AR characteristic curves are shown in Figure 15. As $r = 14$ mm, the 3 dB AR bandwidth is larger and the value of AR is smaller. As the radius decreases, the AR is further reduced. However, the 3 dB AR bandwidth is

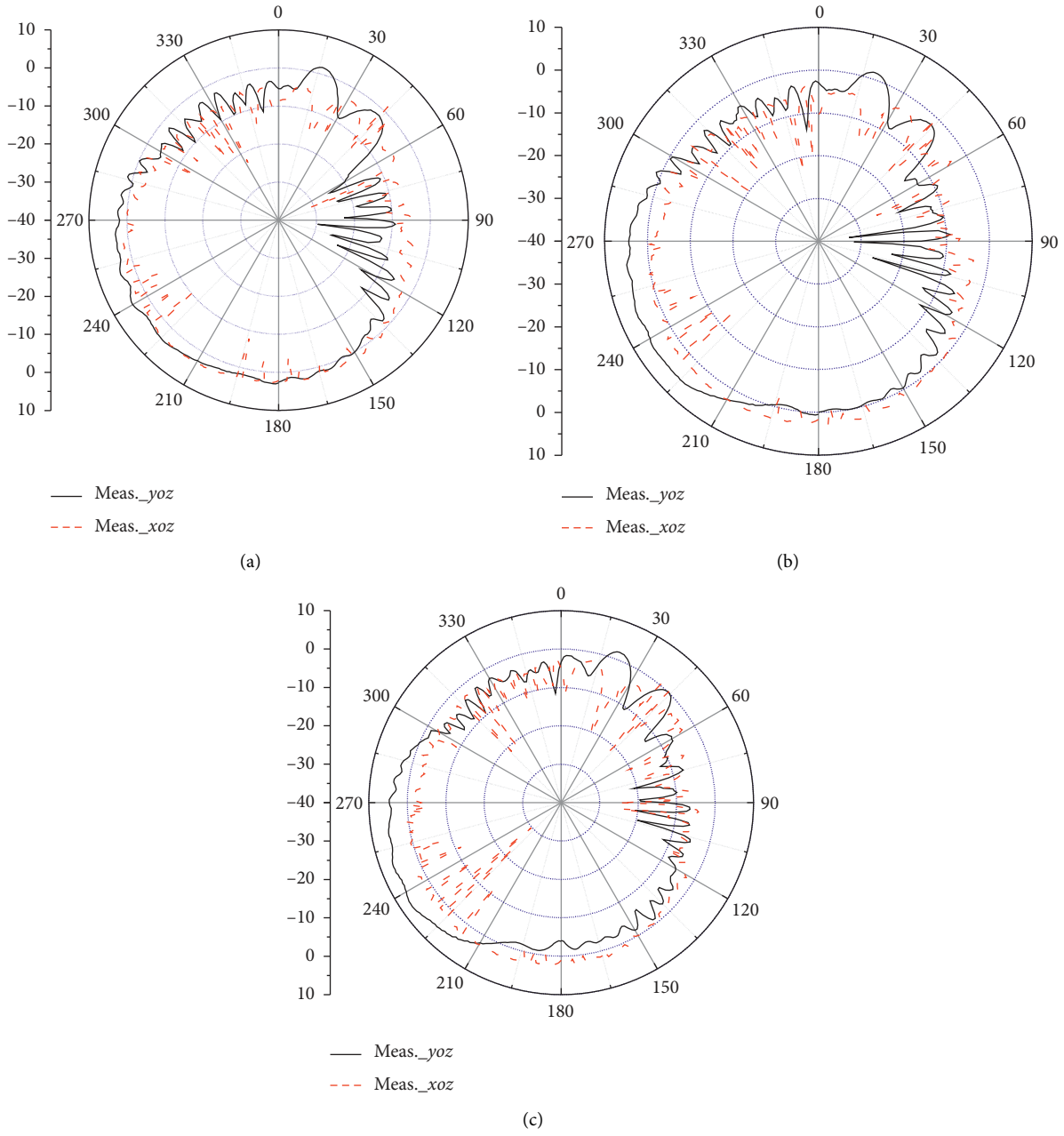

FIGURE 11: The measured CP radiated patterns on *xoz* plane and *yoz* plane, respectively. (a) 6 GHz. (b) 6.5 GHz. (c) 7 GHz. The solid lines correspond to the *yoz* plane, while the dashed lines correspond to the *xoz* plane.

decreased at the same time. When the radius r increases to 1.9 mm, the AR is decreased sharply. At the same time, the 3 dB AR bandwidth is also decreased sharply.

When the length of the loaded inverted L-shaped microstrip is changed, the corresponding AR characteristics are shown in Figure 16. The length of the arm connecting the inverted L-shaped microstrip and the radiation patch remains unchanged. When the other arm length L_3 is increased from 3 mm to 6 mm in step of 1 mm, the AR characteristics of the antenna are influenced obviously. On the condition of $L_3 = 5$ mm, the AR value is the smallest and the bandwidth is the widest. With the increment of L_3, the AR value is decreased and the 3 dB AR bandwidth is decreased at the same time. When the length of L_3 is decreased from 5 mm, the AR characteristic is deteriorated, and the 3 dB axis ratio bandwidth is decreased also sharply.

When the radius R of the cutting-out quarter circle is increased from 7 mm to 8.5 mm by a step of 0.5 mm, the 3 dB AR characteristic curves are shown in Figure 17. If the radius R is small ($R = 7$ mm) or large ($R = 8.5$ mm), the

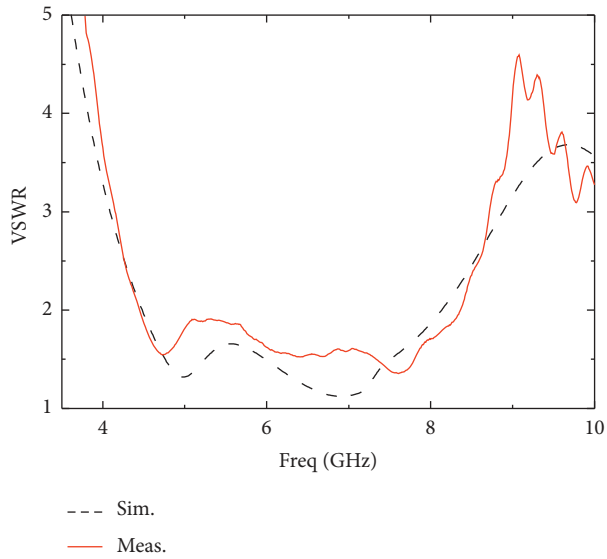

Figure 12: Measured VSWR of the CP antenna. Solid line shows the measured result, while the dashed line shows the simulation result.

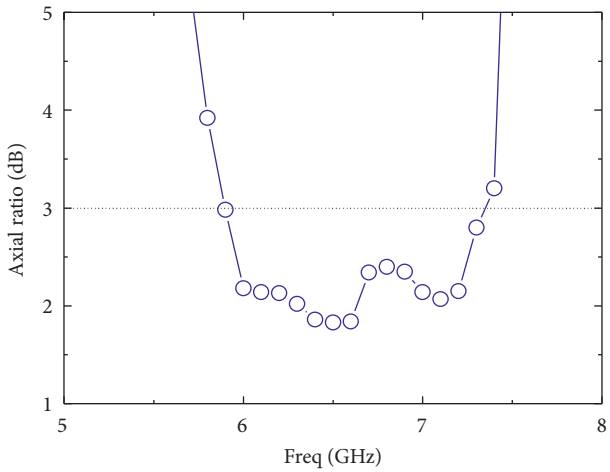

Figure 13: Measured results of the AR curve.

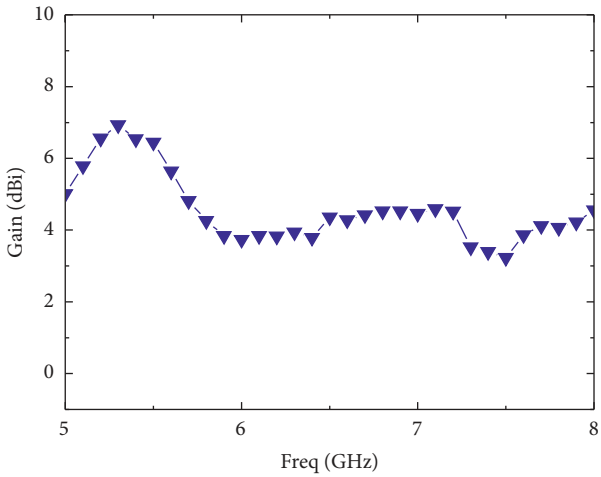

Figure 14: Measured results of the antenna gain.

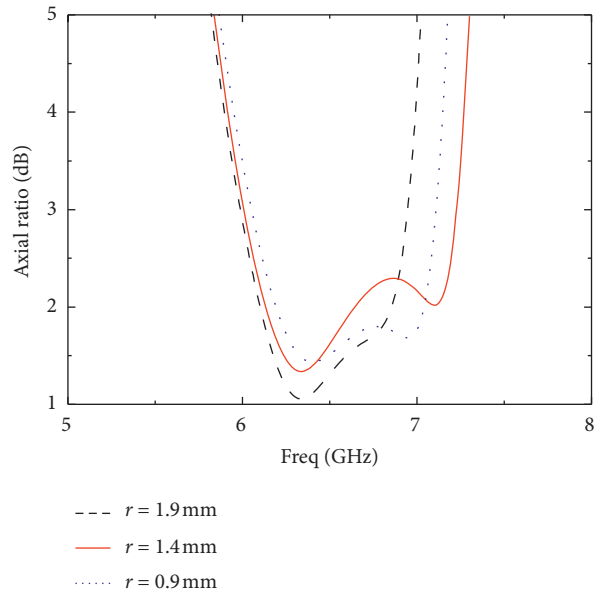

Figure 15: Simulation results of AR with different annular-ring slot radius r including $r = 0.9$ mm (dotted line), $r = 1.4$ mm (solid line), and $r = 1.9$ mm (dashed line).

AR is changed drastically, and the CP performance is deteriorated. The AR of the low frequency is increased immediately with R decreasing. At the same time, the working frequency band shifts to the left. The AR of the high frequency is increased with R increasing. Meanwhile, the working frequency band shifts to the right. Based on the results in Figure 17, the optimal result corresponds to the radius R being 8 mm.

When the slot width of the loaded annular-ring slot is changed, the AR curve is shown in Figure 18. As the slot width is significantly increased, the value of the AR is slightly

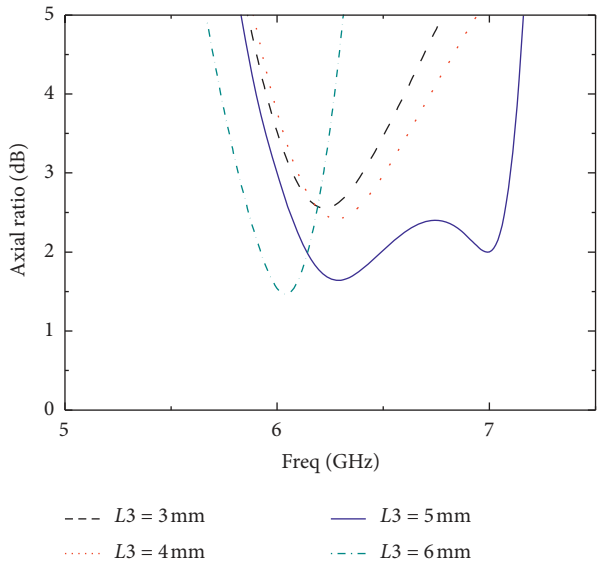

Figure 16: Simulation results of the AR when the inverted L-shaped microstrip length $L3$ is varied from 3 mm to 6 mm, with a step of 1 mm increment.

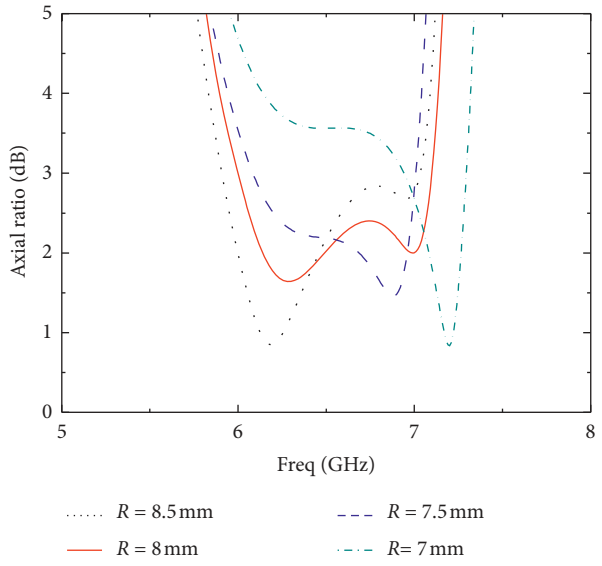

Figure 17: Simulation results of the AR when the cutting-out quarter circle radius R varied from 7 mm to 8.5 mm, with a step of 0.5 mm increment.

increased. But the variation of the AR bandwidth is not obvious. The reflection coefficient is decreased.

It can be found that the radius and the width of the annular-ring slot have little influence on the AR performance based on the above analysis. So, the 3 dB AR bandwidth and the in-band AR value can be tuned slightly. It is worth noting that the position of the annular-ring slot seriously affects the AR performance. The radius of the cutting-out circle and the length of the inverted L-shaped microstrip have obvious impacts on the AR performance. As the size changes, the 3 dB AR bandwidth and the AR value are changed significantly.

For a clear comparison, Table 2 lists the comparison of CP UWB antennas excited by various slots. The key results of the published CP antennas are listed in Table 2. The structure proposed in the paper is also included in Table 2, being one of the most excellent properties among the published results. The antenna impedance bandwidth is relatively extended.

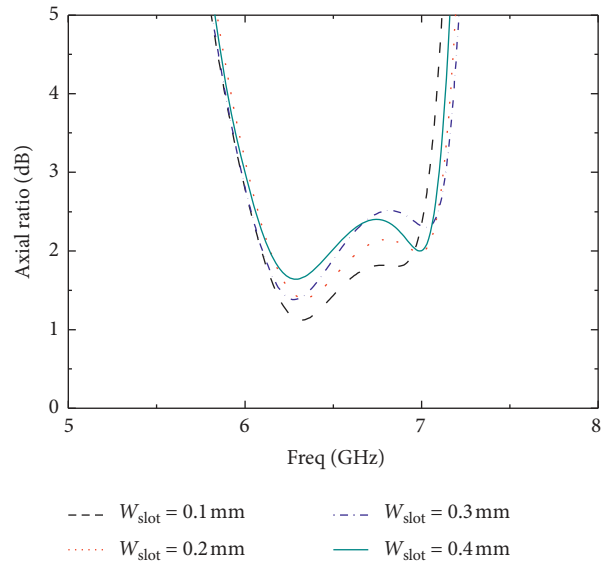

Figure 18: Simulation results of the AR when the annular-ring slot width w_{slot} is varied from 0.1 mm to 0.4 mm, with a step of 0.1 mm increment.

Table 2: Comparison of reference CP UWB microstrip slot antennas.

Ref.	Antenna type	IBW (S11<−10 dB) GHz	3 dB ARBW GHz (fractional band)	Dielectric	Antenna area (mm × mm)	Peak gain (dBi)
[12]	Meander square ring slot	3.15–3.9	−(9%)	RO4003 and FR4	21 × 21	8
[6]	Square ring slot	2.45–3.1	−(6.3%)	FR4	54 × 54	3.3
[13]	Annular-ring slot	2.4–3.034	−(10.5%)	$\varepsilon_r = 4.4$	<90 × 90	4.4
[14]	Annular slot and cross slot	4.7–7.2 2.2–2.6	0.148 (5.92%) 0.160 (2.46%)	$\varepsilon_r = 4.2$	39 × 62	4.1 5.8
[15]	Slot antenna	1.01–3.33	0.55 (32.35%) 0.25 (5.6%)	$\varepsilon_r = 3.2$	70 × 70	2.5 2.5
[16]	Annular slot with linear slot	1.265–1.654 2.446–2.738	0.092 (6.1%) 0.155 (6%)	$\varepsilon_r = 4.2$	80 × 80	5.2 6.3
[17]	Spiral slot	1.437–1.724 2.418–2.907	0.072 (4.45%) 0.093 (3.5%)	$\varepsilon_r = 3.5$	100 × 100	4.4 3.8
[18]	Square slot	2.674–13.124	2 (32.2%)	$\varepsilon_r = 4.4$	60 × 60	4.2
[21]	Square ring slot	1.347–1.533	0.065 (3.4%)	$\varepsilon_r = 4.4$	80 × 80	4.3
[22]	Moon-shaped	2.08–3.75	1.48 (49.3%)	$\varepsilon_r = 4.2$	46.6 × 70	1.6
[23]	Trapezoidal	2.84–4.58	1.4 (36%)	FR4	38 × 40	2
This paper	Annular-ring slot	4.52–8.06	1.4 (21.25%)	FR4	25 × 24	4.59

IBW: impedance bandwidth.

The 3 dB AR absolute bandwidth reaches 1.4 GHz, while the 3 dB AR fractional bandwidth is 21.25% and the peak gain is higher in the small area.

6. Conclusions

A novel UWB CP antenna is proposed and implemented in the paper. In the antenna, the structure with the cutting-off quarter circle on the corner of the radiation patch is intentionally designed on the FR4 substrate. The annular-ring slot and the inverted L-shaped microstrip are integrated in the structure to implement the CP radiation. The tapered-shaped microstrip is used to connect the radiating patch and the feed line excited by a single feed for achieving a good impedance matching in the wider frequency band. Finally, the key structural parameters are discussed on the effects of the polarization performance, separately. This UWB CP antenna can be used in wireless communication systems, such as unmanned aircraft and wireless sensors.

Data Availability

The data that support the findings of this study are available from the first author or corresponding author upon reasonable request.

Conflicts of Interest

The authors declare that there are no conflicts of interest regarding the publication of this paper.

Acknowledgments

This work was supported by the National Natural Science Foundation of China (61774078), the Fujian Natural Science Foundation Project (2019J01718), and the Natural Science Foundation Program (Emphasis) (2020JD2042).

References

[1] T.-G. Ma and C.-H. Tseng, "An ultrawideband coplanar waveguide-fed tapered ring slot antenna," *IEEE Transactions on Antennas and Propagation*, vol. 54, no. 4, pp. 1105–1110, 2006.

[2] Z. N. Low, J. H. Cheong, and C. L. Law, "Low-cost PCB antenna for UWB applications," *IEEE Antennas and Wireless Propagation Letters*, vol. 4, pp. 237–239, 2005.

[3] C. C. Chung and M. R. Kamarudin, "Novel design of circular UWB antenna," in *Proceedings of the 2009 Asia Pacific Microwave Conference*, pp. 1977–1979, IEEE, Singapore, Singapore, December 2009.

[4] A. J. Poelman, "Virtual polarization adaptation a method of increasing the detection capability of a radar system through polarization-vector processing," *IEE Proceedings-F Radar and Signal Processing*, vol. 128, no. 10, pp. 261–270, 1981.

[5] R. F. Xue and S. S. Zhong, "Survey and progress in circular polarization technology of microstrip antennas," *Chinese Journal of Radio Science*, vol. 17, no. 4, pp. 331–336, 2002.

[6] J.-S. Row, "The design of a squarer-ring slot antenna for circular polarization," *IEEE Transactions on Antennas and Propagation*, vol. 53, no. 6, pp. 1967–1972, 2005.

[7] Z.-Q. Liu, Y.-S. Zhang, Z. Qian, Z. P. Han, and W. Ni, "A novel broad beamwidth conformal antenna on unmanned aerial vehicle," *IEEE Antennas and Wireless Propagation Letters*, vol. 11, pp. 196–199, 2012.

[8] G. Collins, "Effect of reflecting structures on circularly polarized TV broadcast transmission," *IEEE Transactions on Broadcasting*, vol. 25, no. 1, pp. 5–13, 1979.

[9] A.-S. Kaddour, S. Bories, A. Bellion, and C. Delaveaud, "3-D-printed compact wideband magnetoelectric dipoles with circular polarization," *IEEE Antennas and Wireless Propagation Letters*, vol. 17, no. 11, pp. 2026–2030, 2018.

[10] C. Shu, J. Wang, S. Hu et al., "A wideband dual-circular-polarization horn antenna for mmwave wireless communications," *IEEE Antennas and Wireless Propagation Letters*, vol. 18, no. 9, pp. 1726–1730, 2019.

[11] A. Altaf and M. Seo, "A tilted-D-shaped monopole antenna with wide dual-band dual-sense circular polarization," *IEEE Antennas and Wireless Propagation Letters*, vol. 17, no. 12, pp. 2464–2468, 2018.

[12] A. Buffi, R. Caso, M. R. Pino, P. Nepa, and G. Manara, "Single-feed circularly polarised aperture-coupled square ring slot microstrip antenna," *Electronics Letters*, vol. 46, no. 4, pp. 268-269, 2010.

[13] J.-Y. Sze, C.-I. G. Hsu, M.-H. Ho, Y.-H. Ou, and M.-T. Wu, "Design of circularly polarized annular-ring slot antennas fed by a double-bent microstripline," *IEEE Transactions on Antennas and Propagation*, vol. 55, no. 11, pp. 3134–3139, 2007.

[14] Y. Shao and Z. Chen, "A design of dual-frequency dual-sense circularly-polarized slot antenna," *IEEE Transactions on Antennas and Propagation*, vol. 60, no. 11, pp. 4992–4997, 2012.

[15] Y. Y. Chen and Y. C. Jiao, "Dual-band dual-sense circularly polarized slot antenna with a C-shaped grounded strip," *IEEE Antennas Wireless Propagation Letters*, vol. 10, pp. 915–918, 2011.

[16] X. Bao and M. J. Ammann, "Dual-frequency dual-sense circularly-polarized slot antenna fed by microstrip line," *IEEE Transactions on Antennas and Propagation*, vol. 56, no. 3, pp. 645–649, 2008.

[17] X. L. Bao and M. J. Ammann, "Monofilar spiral slot antenna for dual-frequency dual-sense circular polarization," *IEEE Transactions on Antennas and Propagation*, vol. 59, no. 8, pp. 3061–3065, 2011.

[18] J. Pourahmadazar, C. Ghobadi, J. Nourinia, N. Felegari, and H. Shirzad, "Broadband CPW-fed circularly polarized square slot antenna with inverted-L strips for UWB applications," *IEEE Antennas and Wireless Propagation Letters*, vol. 10, pp. 369–372, 2011.

[19] S. Matsuzawa and K. Ito, "Circularly polarised printed antenna fed by coplanar waveguide," *Electronics Letters*, vol. 32, no. 22, pp. 2035-2036, 1996.

[20] E. A. Soliman, S. Brebels, E. Beyne, and G. Vandenbosch, "Circularly polarised aperture antenna fed by CPW and built in the MCM-D technology," *Electronics Letters*, vol. 35, no. 4, pp. 250-251, 1999.

[21] K. Wong, C. Huang, and W. Chen, "Printed ring slot antenna for circular polarization," *IEEE Transactions on Antennas and Propagation*, vol. 50, no. 1, pp. 75–77, 2002.

[22] B. Hu, Nasimuddin, and Z. Shen, "Broadband circularly polarized moon-shaped monopole antenna," *Microwave and Optical Technology Letters*, vol. 57, no. 5, pp. 1135–1139, 2015.

[23] R. John, Nasimuddin, and A. Alphones, "Wideband circularly polarized modified trapezoida*L*-shaped monopole antenna," in *Proceedings of the 2015 IEEE International Symposium on Antennas and Propagation & USNC/URSI National Radio Science Meeting*, pp. 1946-1947, IEEE, Vancouver, BC, Canada, July 2015.